

Synthesis of Porous Si/SiO₂/C Particles as Anode Materials of Lithium-Ion Batteries

Chengmao Xiao, Ning Du, Deren Yang*

State Key Lab of Silicon Materials and Department of Materials Science and Engineering, Cyrus Tang Center for Sensor Materials and Applications, Zhejiang University, China

*Corresponding author: Deren Yang, State Key Lab of Silicon Materials and Department of Materials Science and Engineering, Cyrus Tang Center for Sensor Materials and Applications, Zhejiang University, Hangzhou 310027, People's Republic of China, E-mail: mseyang@zju.edu.cn

Received Date: January 26, 2014 Accepted Date: February 13, 2014 Published Date: March 11, 2014

Citation: Deren Yang (2014) Synthesis of Porous Si/SiO₂/C Particles as Anode Materials of Lithium-Ion Batteries. J Nanotech Smart Mater 1: 1-4

Abstract

We demonstrate the synthesis of the porous Si/SiO₂/C particles by the oxidation of Mg₂Si and subsequent deposition of carbon layers. When used as anode materials of lithium-ion batteries, the porous Si/SiO₂/C particles deliver a capacity of 550 mAhg⁻¹ after 30 cycles at a current of 800 mA_g-1, which is better than bulk Si particles. The enhanced electrochemical performance is ascribing to the porous and core-shell structures. Moreover, the silicon dioxides layer is beneficial to the stability of the SEI film, and the carbon layer and the porous structures can buffer the volume change during the charge/discharge process, which may be responsible the enhanced performance.

Introduction

Silicon (Si) is one of the most promising anode materials for next-generation lithium-ion (Li-ion) batteries, which has the highest specific capacity of ~4200 mAhg⁻¹ [1]. However, there are two main drawbacks of Si anode materials: the first one is the large volume expansion up to nearly 400 % based on the formation of Li_{4.4}Si during alloying/de-alloying processes, resulting in cracking and pulverization of the electrode and badly contacted with the currents, which makes it hardly to retain the long cyclic performance [2-4]; the other one is the unstable solid electrolyte interface (SEI) formation during the lithium ion insertion and deinsertion process [5-7]. Recently, different Si nano/micro- structures such as nanotubes [8-9], nanorods [10], nanowires [11-13], nanoparticles [14-15], thin films [16-17], and mesoporous structures [18-20] has been synthesized to improve the cyclic performance. Meanwhile, the protection of the anode from the directly contacting with the electrolyte to form stable SEI film has been approved to be another choice to enhance the cyclic performance. SiO₂, the natural silicon oxide, has

been chosen to act as the separation [21-26] between the anode and the electrolyte to stabilize SEI films. The SiO₂ layer is also easy to form and could accommodate the volume expansion during charge/discharge process. Cui's group synthesized a novel double-walled Si nanotube with a thin SiO₂ layer outside, leading to a stable SEI film [9]. The Si/SiO₂ nanotube shows excellent cyclic performance over 6000 cycles. However, most SiO₂-coated Si particles show very low capacity even at a low current due to the non-conductivity of the SiO₂ layer. For example, Su et al. [24] synthesized a double shell Si/SiO₂/C nanocomposites, in which the SiO₂ was coated by decomposed with Li₂SO₄. They showed that both of the SiO₂ and the carbon layers could accommodate the volume expansion of Si, leading to good cycling stability. A reversible capacity of 800 mAhg⁻¹ is achieved at a very low current of 50 mA_g-1 after 30 cycles. However, the rate capacity is dissatisfactory due to the non-conductive of the SiO₂. Therefore, it is a great challenge to further improve cycling performance by using the above-mentioned strategies.

Herein, we report a simple, convenient way to synthesize porous Si/SiO₂/C particles. A comparable capacity of 550 mAhg⁻¹ is achieved even at a high current of 800 mA_g-1 after 30 cycles with a relatively thick SiO₂ layer. The double layers of the SiO₂ and carbon can not only buffer the volume expansion, but also form a stable SEI film.

Experimental

Synthesis of porous Si/SiO₂/C particles

Mg₂Si (purity, >90%) was purchased from Zhejiang YHL New Energy Material Corporation. At first, 0.5 g Mg₂Si was annealed at 700 °C in the air for 20 h in a tube furnace. After cooling down to room temperature, the product was treated by the hydrochloric acid (HCl) solution (0.2 molL⁻¹) for 30 min. After washed with deionized water and ethanol for three times, the product was centrifuged and collected. Finally, the product was dried at 80 °C for 6 h in the air. For coating of a carbon layer, 0.2 g products was annealed at 600 °C for 2 h in a mix gas flowing (C₂H₂:Ar = 1:10, volume ratio) in a tube furnace.

Characterization

A Rigaku D/max-ga x-ray diffractometer with graphite monochromatized Cu K α radiation ($\gamma = 1.54178 \text{ \AA}$) was used to detect the samples. The morphologies and the structures were characterized by the scanning electron microscopy (SEM, Hitachi S4800) and transmission electron microscopy (TEM, JEM-200 CX, 160 kV) and high-resolution transmission electron microscopy (HRTEM, JEOL JEM-2010).

Electrochemical performance

Electrochemical performance was carried out using the half-cell testing method with the lithium metal as the counter and reference anode. Briefly, Si/SiO₂/C, acetylene black (AB), polyvinylidene fluoride (PVDF), with a mass ratio of 75: 15: 10, were mixed and dissolved in the N-methyl-2-pyrrolidone (NMP) to get an uniform slurry. After pasting on the copper foils and dried at 120 °C for 12 h under vacuum, the cells were assembled in an argon-filled glove box. The electrolyte was 1 M LiPF₆ dissolved in a mixture of ethylene carbonate (EC) and diethyl carbonate (DEC) with the volume ratio of EC:DEC = 1:1. An Arbin BT 2100 system was used for the electrochemical performance. All cells were cycled in the range of 0.01~1.5 V at different current densities.

Electrochemical performance

Fig.1 is the evolution of the XRD patterns from Mg₂Si to porous Si/SiO₂/C composites. The black curve (a) represents the pure Mg₂Si materials. After annealed at 700 °C for 20 h in the air, Mg₂Si has completely transformed into MgO, Si and SiO₂, which can be proved by the peaks in curve b (JCPDS file: 27-1402 and 45-0946). After treated with HCl, MgO is completely removed, which can be identified in curve c. Considering the SiO₂ and carbon layer are both amorphous, which can't be reflected in XRD patterns.

Figs.2a,b and c show SEM images of the porous Si/SiO₂/C particles with different magnification. It can be seen from the low-magnified SEM image (Fig. 2a) that the size of the particles is 5~10 μm . In the high-magnified SEM images (Figs. 2b and c), many pores in the particles can be observed with the size of 50~200 nm. Fig. 2d shows the EDX pattern of the products. It can be seen that the elements Cu, Si, O and C can be detected, which are originated from the Cu substrate and Si/SiO₂/C particles, respectively. In order to further identify the SiO₂ and carbon layer, TEM and HRTEM analysis were

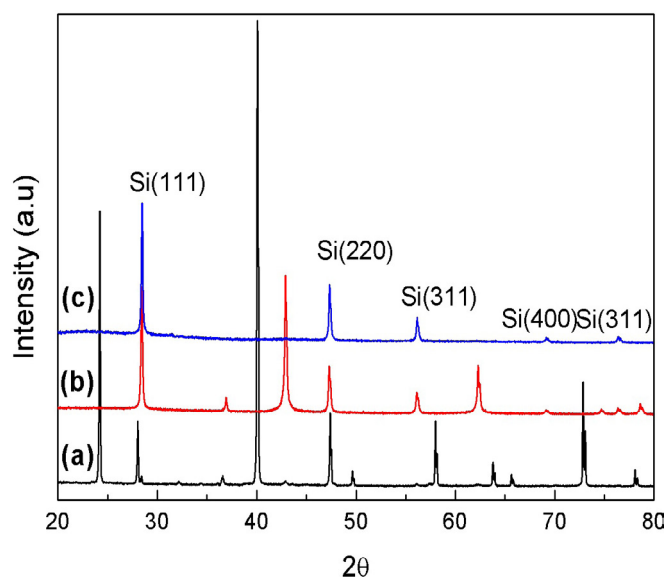


Figure 1: XRD patterns of the products along with the synthetic process: (a) Mg₂Si; (b) the sample annealed at 700 °C for 20 h in air; (c) after washing by HCl solution for 4 h.

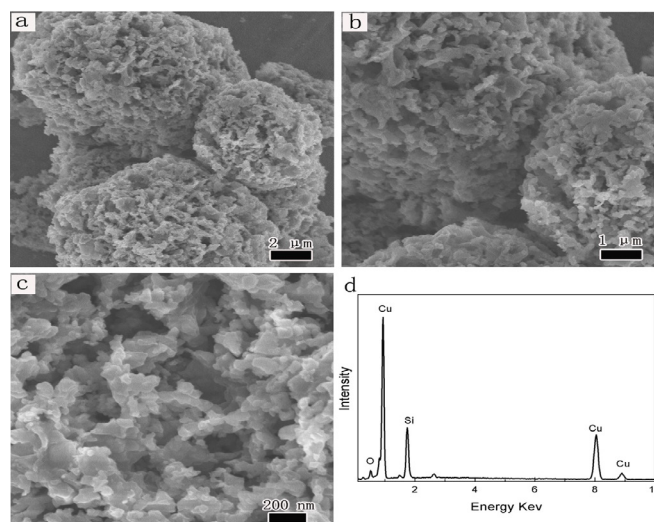


Figure 2: SEM images (a), (b), (c) and EDX pattern (d) of the Si/SiO₂/C particles

employed. From the low-magnified TEM image (Fig. 3a), we can see that the particles are composed of small particles ranging from 50 to 200 nm which are connected with each other to form a porous structure. Figs. 3b and c show the high-magnified TEM images of the porous Si/SiO₂/C particles. The strong contrast between the core and outer layer indicates that an amorphous layer exists on the surface of the Si particles. The thickness of the amorphous layer is about 5~20 nm. It is well known that Si could be easily oxidized even at room temperature. The generated SiO₂ layer will prevent the inner silicon from oxidation, so the thickness of the SiO₂ is usually very thin at room temperature. In this case, the high annealing temperature could offer large driving force which would lead to continuous oxidation. Fig. 3d shows the HRTEM image of a porous Si/SiO₂/C particle. As can be seen, the amorphous layer is composed of a SiO₂ layer and carbon layer, respectively. To further characterize the element distribution of the porous Si/SiO₂/C particles, the EDX mapping was employed (Fig.4).

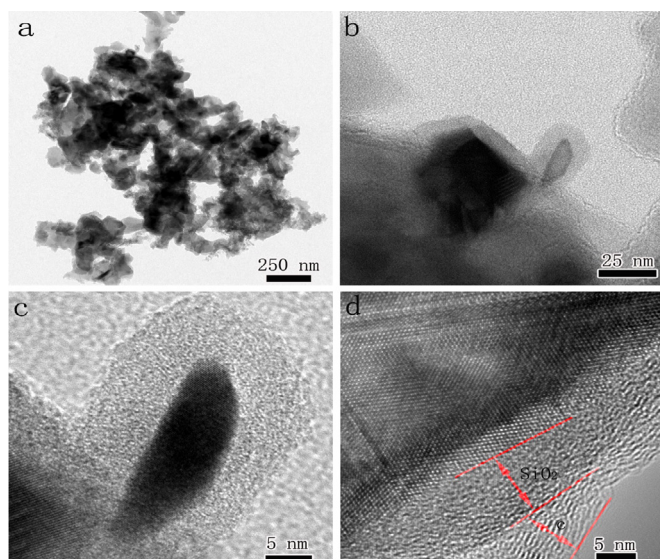


Figure 3: TEM (a), (b), (c) and HRTEM images (d) of the Si/SiO₂/C particles.

It can be seen that Si and O show uniform distribution in a Si/SiO₂/C particle, while C only exists on the surface of the particle. This indicates that the oxidation of the Si is uniform, while the carbon doesn't penetrate into internal of the porous particle.

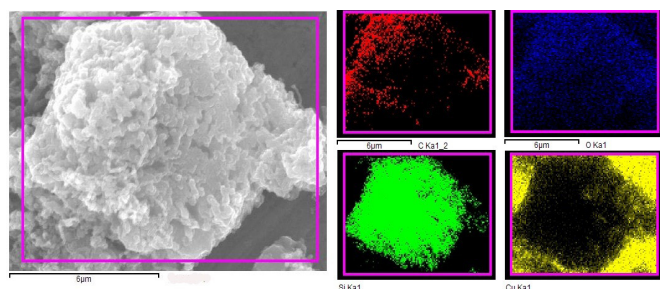


Figure 4: Element mapping of a porous Si/SiO₂/C particles.

Motivated by the core-shell structures, the electrochemical performance of porous Si/SiO₂/C particles is tested as anode materials of Li-ion batteries. Fig. 5a is the cyclic voltammograms of the porous Si/SiO₂/C particles at a scanning rate of 0.1 mVs⁻¹. A distinct broad peak at ~0.8 V in the first charge profile is ascribed to the formation of SEI films on the surface of the active particles [24]. Below 0.2 V, a sharp reduction peak represents the insertion of lithium ion into Si, which is the typical anode peak of Si. After the first cycle, two oxidation peaks around 0.3 and 0.5 V, and a new reduction peak near 0.2 V are observed. All the multiple peaks are the representative processes of alloying and dealloying for amorphous silicon. Fig. 5b shows the first and second charge/discharge curves of the porous Si/SiO₂/C particles measured at 0.2 C in the voltage range of 0.01~1.5 V. It can be seen that the charge and discharge platforms are consistent with the peaks in the CV curves. The first discharge capacity of the porous Si/SiO₂/C particles is 3356.5 mAhg⁻¹, while the first charge capacity is 2107 mAhg⁻¹, resulting in the initial Coulombic efficiency of 62.8%. The relatively low initial Coulombic efficiency is mainly due to the large surface area and the existence of SiO₂ layer. Fig. 6a shows the Coulombic efficiency and discharge/charge capacity versus cycling numbers. It can be seen that the Coulombic efficiency increases to higher than 95% after 10 cycles

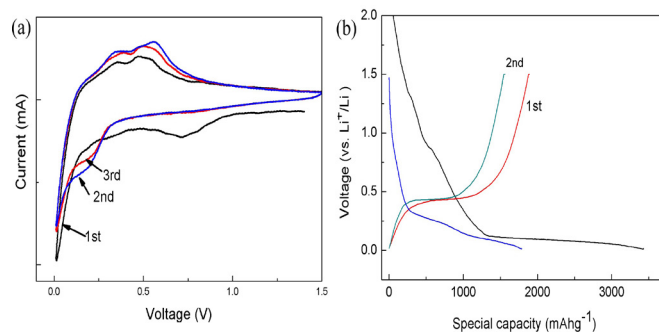


Figure 5: (a) First three CV plots of the porous Si/SiO₂/C particles at the scan rate of 0.1 mVs⁻¹; (b) first two charge and discharge curves for the porous Si/SiO₂/C particles at the current of 800 mA g⁻¹.

and even nearly 100% after 20 cycles. A reversible discharge capacity of 550 mAhg⁻¹ is remained after 30 cycles at a current density of 0.2 C (800 mA g⁻¹), which is better than previous results [23, 24]. The enhanced performance may be attributed to the following two reasons: the co-existence of SiO₂ and C layer could prevent the silicon core from directly contacting with the electrolyte, which may decrease the regeneration of the SEI film [9]; the core-shell and porous structure can accommodate the volume changes during alloying/de-alloying process. Fig. 6b shows the cycling performance for the porous Si/SiO₂/C particles at different current densities. As observed, the specific capacity fades fast along with the increasing current. When the current density recovers to 0.8 Ag⁻¹, the capacity can restore to the previous state, indicating the good rate performance. Even at a very high current density, 3.2 Ag⁻¹, a reversible capacity over 250 mAhg⁻¹ is remained. The good rate capability of the porous Si/SiO₂/C particles is due to the porous structure and the co-existence of SiO₂ and C layer to form a stable SEI film. It is believed that the cycling and rate performance can be further enhanced by adjusting the thickness of the SiO₂ and carbon layer, which is under investigation.

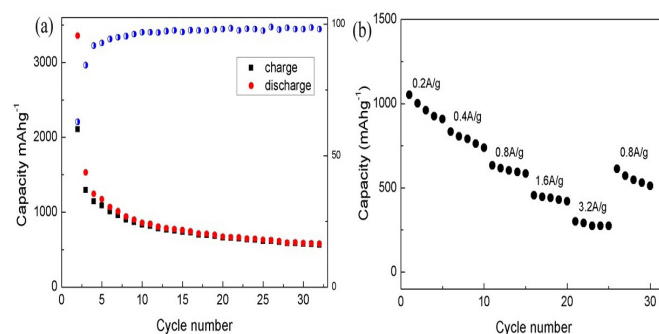


Figure 6: (a) Capacity versus cycling numbers of the porous Si/SiO₂/C particles at the testing current of 800 mA g⁻¹; (b) Rate capability of the porous Si/SiO₂/C particles.

Conclusion

In summary, the porous Si/SiO₂/C particles were synthesized via the annealing of Mg₂Si and subsequent carbon coating. When used as anode materials of Li-ion batteries, a reversible capacity over 550 mAhg⁻¹ is retained at the current of 800 mA g⁻¹ after 30 cycles. The cycling and rate performance is improved compared to bulk Si materials. The SiO₂ and carbon layer can not only protect the Si from directly contacting with the electrolyte, but also acts as the buffer to release

the volume change during the charge/discharge process, which may be responsible for the enhanced performance.

Acknowledgement

The authors would like to appreciate the financial supports from the 863 Project (No. 2011AA050517), NSFC (No. 51002133) and Innovation Team Project of Zhejiang Province (2009R50005).

References

- 1) Szczecch JR, Jin S (2011) Nanostructured silicon for high capacity lithium battery anodes. *Energy Environ. Sci* 4: 56-72.
- 2) Teki R, Datta MK, Krishnan R, Parker TC, Lu TM, et al. (2009) Nanostructured silicon anodes for lithium ion rechargeable batteries. *Small* 5: 2236-2242.
- 3) Kang Z, Liu v, Lee ST (2011) Small-sized silicon nanoparticles: new nanolights and nanocatalysts. *Nanoscale* 3: 777-791.
- 4) Yoo JK, Kim J, Jung YS, Kang K (2012) Scalable Fabrication of Silicon Nanotubes and their Application to Energy Storage. *Adv. Mater* 24: 5452-5456.
- 5) Beaulieu LY, Eberman KW, Turner RL, Krause LJ, Dahn JR (2001) Colossal Reversible Volume Changes in Lithium Alloys. *Solid State Lett* 4: A137-A140.
- 6) Hatchard TD, Dahn JR (2004) In Situ XRD and Electrochemical Study of the Reaction of Lithium with Amorphous Silicon. *J. Electrochem. Soc* 151: A838-A842.
- 7) Aurbach D (2000) Review of selected electrode-solution interactions which determine the performance of Li and Li ion batteries. *J. Power Sources* 89: 206-218.
- 8) Song T, Xia J, Lee JH, Lee DH, Kwon MS, et al. (2010) Arrays of Sealed Silicon Nanotubes As Anodes for Lithium Ion Batteries. *Nano Lett* 10: 1710-1716.
- 9) Wu H, Chan G, Choi JW, Ryu Ill, Yao Y, et al. (2011) Interconnected Silicon Hollow Nanospheres for Lithium-Ion Battery Anodes with Long Cycle Life. *Nano Lett* 11: 2949-2954.
- 10) Ghassemi H, Au M, Chen N, Heiden PA, Yassar RS (2011) In situ electrochemical lithiation/delithiation observation of individual amorphous Si nanorods. *ACS. Nano* 10: 7805-7811.
- 11) Huang R, Fan X, Shen W, Zhu J (2009) Carbon-coated silicon nanowire array films for high-performance lithium-ion battery anodes. *Appl. Phys. Lett* 95: 133119.
- 12) Cui LF, Yang Y, Hsu CM, Cui Y (2009) Carbon-silicon core-shell nanowires as high capacity electrode for lithium ion batteries. *Nano. Lett* 9: 3370-3374.
- 13) Wang W, Kumta PN (2010) Nanostructured hybrid silicon/carbon nanotube heterostructures: reversible high-capacity lithium-ion anodes. *ACS. Nano* 4: 2233-2241.
- 14) Mazouzi D, Lestriez B, Roue L, Guyomard D (2009) Silicon composite electrode with high capacity and long cycle life. *Electrochem. Solid-State Lett* 12: A215-A218.
- 15) Li H, Huang X, Chen L, Wu Z, Liang Y (1999) A high capacity nano Si composite anode material for lithium rechargeable batteries. *Electrochem. Solid-State Lett* 2: 547-549.
- 16) Hwang CM, Lim CH, Yang JH, Park JW (2009) Electrochemical properties of negative SiMox electrodes deposited on a roughened substrate for rechargeable lithium batteries. *J. Power Sources* 194: 1061-1067.
- 17) Ding N, Xu J, Yao YX, Wegner G, Fang X, et al. (2009) Determination of the diffusion coefficient of lithium ions in nano-Si. *Solid State Ionics* 180: 222-225.
- 18) Kim H, Han B, Choo J, Cho J (2008) Three-Dimensional Porous Silicon Particles for Use in High-Performance Lithium Secondary Batteries. *Angew. Chem. Int. Ed* 47: 10151-10154.
- 19) Jia H, Gao P, Yang J, Wang J, Nuli Y, et al. (2011) Novel Three-Dimensional Mesoporous Silicon for High Power Lithium-Ion Battery Anode Material. *Adv. Energy Mater* 1: 1036-1039.
- 20) Bang BM, Lee JI, Kim H, Cho J, Park S (2012) High-Performance Macroporous Bulk Silicon Anodes Synthesized by Template-Free Chemical Etching. *Adv. Energy Mater* 2: 878-883.
- 21) Lu Z, Zhang L, Liu X (2010) Microstructure and electrochemical performance of Si-SiO₂-C composites as the negative material for Li-ion batteries. *J. Power Sources* 195: 4304-4307.
- 22) Wang J, Zhao H, He J, Wang C, Wang J (2011) Nano-sized SiOx/C composite anode for lithium ion batteries. *J. Power Sources* 196: 4811-4815.
- 23) Gomez-Camer JL, Morales J, Sanchez L (2011) Anchoring Si nanoparticles to carbon nanofibers: an efficient procedure for improving Si performance in Li batteries. *J. Mater. Chem* 21: 811-818.
- 24) Su L, Zhou Z, Ren M (2010) Core double-shell Si@ SiO₂@ C nanocomposites as anode materials for Li-ion batteries. *Chem. Commun* 46: 2590-2592.
- 25) Saint J, Morcrette M, Larcher D, Laffont L, Beattie S, et al. (2007) Towards a fundamental understanding of the improved electrochemical performance of silicon-carbon composites. *Adv. Funct. Mater* 17: 1765-1774.
- 26) Hu YS, Rezan DC, Titirici MM, Muller JO, Schlogl R, et al. (2008) Superior Storage Performance of a Si@ SiOx/C Nanocomposite as Anode Material for Lithium-Ion Batteries. *Angew. Chem., Int. Ed* 47: 1645-1649.

Submit your manuscript to JScholar journals and benefit from:

- ¶ Convenient online submission
- ¶ Rigorous peer review
- ¶ Immediate publication on acceptance
- ¶ Open access: articles freely available online
- ¶ High visibility within the field
- ¶ Better discount for your subsequent articles

Submit your manuscript at
<http://www.jscholaronline.org/submit-manuscript.php>